Journal of Organometallic Chemistry 693 (2008) 2369–2376

Contents lists available at ScienceDirect

Journal of Organometallic Chemistry

journal homepage: www.elsevier.com/locate/jorganchem

From platina-β-diketones to diacetylplatinum(II) complexes – Synthesis, characterization and structural features

Michael Werner [a], Clemens Bruhn [b], Dirk Steinborn [a,*]

[a] Institut für Chemie – Anorganische Chemie, Martin-Luther-Universität Halle-Wittenberg Kurt-Mothes-Str. 2, D-06120 Halle, Germany
[b] Fachbereich 18, Naturwissenschaften, Abt. Metallorganische Chemie, Universität Kassel, Heinrich-Plett-Strasse 40, D-34132 Kassel, Germany

ARTICLE INFO

Article history:
Received 15 February 2008
Received in revised form 1 April 2008
Accepted 11 April 2008
Available online 16 April 2008

Keywords:
Platinum complexes
Metalla-β-diketones
Acyl complexes
X-ray diffraction analysis
π–π Stacking
Hydrogen bonding

ABSTRACT

The reaction of the electronically unsaturated platina-β-diketone $[Pt_2\{(COMe)_2H\}_2(\mu\text{-}Cl)_2]$ (**1a**) with N⌒N donors led to the formation of diacetyl(hydrido)platinum(IV) complexes $[Pt(COMe)_2Cl(H)(N⌒N)]$ (**2**). By the reaction of these complexes with NaOH in a two-phase system (H_2O/CH_2Cl_2) diacetylplatinum(II) complexes $[Pt(COMe)_2(N⌒N)]$ (N⌒N = bpy, **4a**; 4,4′-Me_2-bpy, **4b**; 4,4′-*t*-Bu_2-bpy, **4c**; 4,4′-Ph_2-bpy, **4d**; 4,4′-*t*-Bu_2-6-*n*-Bu-bpy, **4e**; bpym, **4f**; bpyr, **4g**; phen, **4h**; 4-Me-phen, **4i**; 5-Me-phen, **4j**) were obtained. All complexes were characterized by microanalysis, IR and ^1H and ^{13}C NMR spectroscopy. Additionally, complexes **4a**, **4c**, **4d** and **4e** were characterized by single-crystal X-ray diffraction analysis. The observed variety of packing patterns resulting from π–π stacking and hydrogen bonding is discussed.

1. Introduction

Metalla-β-diketones are hydroxycarbene complexes being stabilized by an intramolecular O–H···O hydrogen bond to a neighboured acyl ligand. Dinuclear platina-β-diketones $[Pt_2\{(COR)_2H\}_2(\mu\text{-}Cl)_2]$ (**1**), synthesized from hexachloroplatinic acid and trimethylsilyl substituted alkynes, exhibit a unique reactivity due to their electronic unsaturation and their kinetically labile ligand sphere [1]. Thus, the platina-β-diketone **1a** was found to react with a wide variety of bidentate N⌒N, P⌒P, S⌒S, and N⌒O donors in the following reaction sequence (Scheme 1): (i) cleavage of the Pt–Cl–Pt bridges yielding mononuclear platina-β-diketones, (ii) oxidative addition yielding diacetyl(hydrido)platinum(IV) complexes **2** and (iii) reductive C–H elimination yielding acetyl(chloro)platinum(II) complexes **3** and acetaldehyde. The course of the reactions proved to be strongly dependent on the nature of the L⌒L ligand. With P⌒P ligands for instance, **1a** was found to react yielding complexes **3** even at temperatures <0 °C whereas with N⌒N ligands thermally extraordinarily stable diacetyl(chloro)hydridoplatinum(IV) complexes of type **2** were obtained [2,3]. With bipyridine and phenanthroline ligands the reductive elimination reaction (iii) did not proceed until 150 °C in the solid-state [2,3]. In sharp contrast, the analogous dimethyl complexes $[PtCl(H)Me_2(N⌒N)]$ (N⌒N = bpy; 4,4′-Me_2-bpy; 4,4′-*t*-Bu_2-bpy) decomposed rapidly at 0 °C with reductive elimination of methane [4].

While the reductive C–H elimination of type **2** complexes (Scheme 1, iii) is well documented, only a few type **2** complexes were found to reductive eliminate HCl yielding diacetylplatinum(II) complexes (Scheme 1, iv). Thus, the platina-β-diketone **1a** reacted with 1,4-di-*n*-propyl-1,4-diazabutadiene and *syn*-2-pyridinaldoxime under the formation of the requisite diacetylplatinum(II) complexes as the main and side product, respectively [5,6]. Furthermore, diacetylplatinum(II) complexes with mono- or bidentate *P* ligands were accessible directly from the platina-β-diketone **1a** by its reaction with NaOMe in the presence of the corresponding phosphine (Scheme 2) [7].

Another way to synthesize diacetylplatinum(II) complexes was described by Klinger et al. [8]: The treatment of $[Pt\{C(O)CH_2CH_2CH_2\}(bpy)]$ with CO led to the formation of $[Pt(CO\text{-}n\text{-}Pr)_2(bpy)]$ in a yield of approximately 15% and a polymeric dicarbonyl(bipyridine)platinum(II) species (Scheme 3).

Dimethylplatinum(II) complexes bearing N⌒N ligands like bipyridine were extensively studied in their reactivity towards oxidative addition reactions [9]. The requisite diacetyl platinum(II) complexes let expect a different stability and reactivity because the acetyl ligand is a much weaker σ-donor than the methyl ligand and may also act as a weak π-acceptor. Here we report on straightforward syntheses and characterization of diacetylplatinum(II) complexes having bipyridine and phenanthroline coligands starting from the platina-β-diketone **1a** via diacetyl(hydrido)platinum(IV)

* Corresponding author. Tel.: +49 345 5525620; fax: +49 345 5527028.
E-mail address: dirk.steinborn@chemie.uni-halle.de (D. Steinborn).

0022-328X/$ - see front matter © 2008 Elsevier B.V. All rights reserved.
doi:10.1016/j.jorganchem.2008.04.016

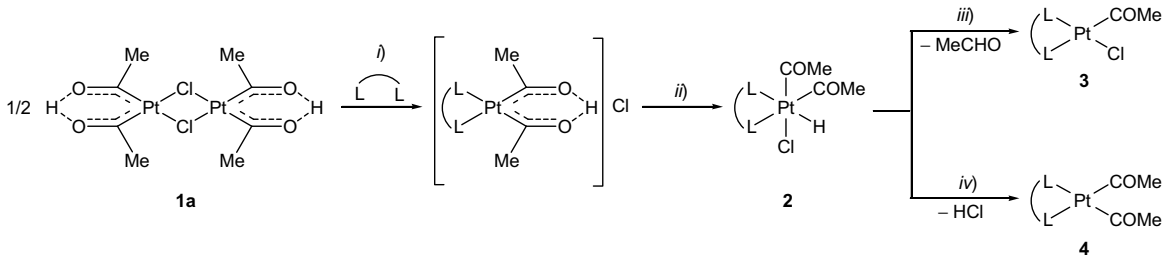

Scheme 1. Reactivity of the platina-β-diketone **1a** towards bidentate ligands.

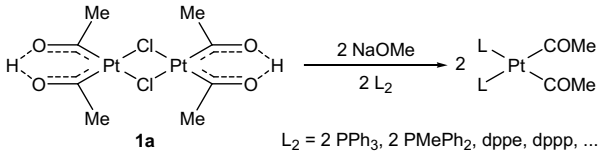

Scheme 2. Synthesis of $[Pt(COMe)_2L_2]$.

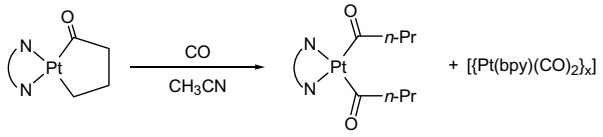

Scheme 3. Synthesis of $[Pt(COPr)_2(bpy)]$.

intermediate complexes (**1a** → **2** → **4**; L⌒L = bpy, phen and derivatives; Scheme 1). Depending on the coligand and cocrystallizing solvate molecules different patterns of π–π stacking as well as different types of hydrogen bonds in crystals of these complexes have been found.

2. Results and discussion

2.1. Synthesis

The dinuclear platina-β-diketone **1a** was found to react with 2,2′-bipyridines (bpy), 1,10-phenanthrolines (phen), 2,2′-bipyrimidine (bpym) and 2,2′-bipyrazine (bpyr) yielding diacetyl(chloro)hydridoplatinum(IV) complexes **2** in good yields of 75–90% [3,10]. When reacting with NaOH in a two-phase mixture (methylene chloride/water), complexes **2** were found to undergo smoothly a reductive HCl elimination yielding diacetylplatinum(II) complexes **4** (Scheme 4). The immediate change of colour from yellow to red when adding an aqueous solution of NaOH to solutions of complexes **2** in CH_2Cl_2 exhibited that the reactions proceeded within seconds at room temperature. Complexes **4a**–**j** have been isolated after recrystallizing from CH_2Cl_2/*n*-pentane in moderate to good yields (60–85%). The intensive red (**4a**, **4d**, **4e**, **4f**, **4g**) and orange coloured (**4b**, **4c**, **4h**, **4i**, **4j**) powdery complexes proved to be air and moisture stable. To remove traces of water in the resulting products, the complexes **4** were dried in vacuum over P_4O_{10} for several days. Their identities were unambiguously confirmed by microanalysis, NMR (^1H, ^{13}C) and IR spectroscopy. Additionally, crystals suitable for X-ray diffraction analysis were obtained for complexes **4a**, **4c**, **4d** and **4e**.

2.2. Spectroscopic characterization

^1H and ^{13}C NMR spectra of complexes **4a**–**j** are fully consistent with the constitution of the complexes given in Scheme 4. Selected NMR spectroscopic data are shown in Table 1. As comparison of the NMR parameters of the diacetylplatinum(II) complexes having substituted bipyridine ligands (**4a**–**d**) revealed, the different 4/4′ substitution (H, Me, *t*-Bu, Ph) do not have any significant influence on NMR parameters of the acetyl ligands. In complexes with asymmetrically substituted N⌒N ligands (**4e**, **4i**, **4j**) the two acetyl ligands are chemically inequivalent. The 6-*n*-butyl substituent in **4e** gives rise to two sets of signals for the two acetyl signals both in the ^1H and ^{13}C NMR spectrum. In the case of the 4- and 5-methyl substituted phenantrolines (**4i**, **4j**) only the chemical shifts of the directly to platinum-bound carbon atoms differ slightly. The signals of the methyl groups ($COCH_3$) are isochronous.

Overall, in all complexes the H and C chemical shifts of the acetyl ligands are in a narrow range. Even the chemical shifts of the directly platinum-bound carbon atoms differ by 6.5 ppm only. The magnitude of $^1J_{Pt,C}$ coupling constants of the non-substituted "par-

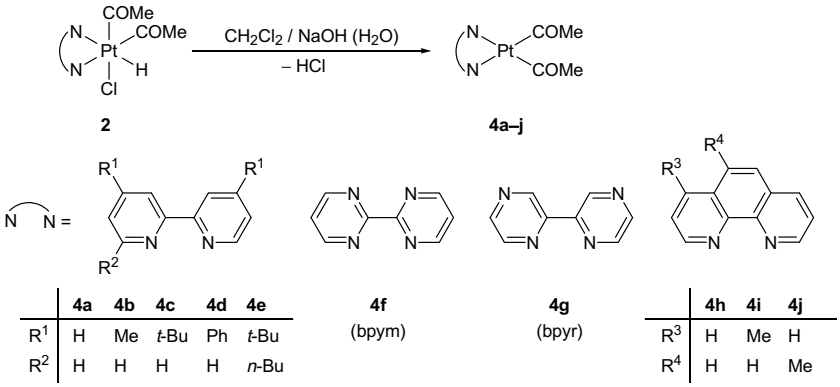

	4a	4b	4c	4d	4e
R^1	H	Me	*t*-Bu	Ph	*t*-Bu
R^2	H	H	H	H	*n*-Bu

	4h	4i	4j
R^3	H	Me	H
R^4	H	H	Me

Scheme 4. Synthesis of diacetylplatinum(II) complexes **4**.

Table 1
Selected NMR spectroscopic parameters of [Pt(COCH$_3$)$_2$(N⌒N)] (**4a–j**) (δ in ppm, J in Hz)

	N⌒N	CH_3		Pt–C
		δ_H ($^3J_{Pt,H}$)	δ_C ($^2J_{Pt,C}$)	δ_C ($^1J_{Pt,C}$)
4a	bpy	2.34 (22.7)	44.4 (371)	230.1 (1269)
4b	4,4′-Me$_2$-bpy	2.21 (23.7)	44.4 (370)	230.6 (1265)
4c	4,4′-*t*-Bu$_2$-bpy	2.26 (24.3)	44.4 (374)	231.3 (1263)
4d	4,4′-Ph$_2$-bpy	2.28 (23.8)	44.4 (370)	230.4 (1262)
4e	4,4′-*t*-Bu$_2$-6-*n*-Bu-bpy	2.17 (24.4)	42.2 (378)	225.8 (1250)
		2.27 (20.5)	44.7 (358)	232.8 (1244)
4f	bpym	2.32 (28.0)	44.2 (386)	226.6 (1244)
4g	bpyr	2.33 (27.8)	44.0 (385)	226.3 (1296)
4h	phen	2.40 (21.2)	44.6 (385)	230.1 (1274)
4i	4-Me-phen	2.32 (25.1)	44.5 (386)	227.7
				227.8
4j	5-Me-phen	2.32 (25.3)	44.5 (387)	227.2
				227.8

ent" ligands was found to increase roughly parallel with the squared LUMO coefficient at the N-atoms of the N⌒N ligands [11]: **4f** (N⌒N = bpym, 1244 Hz) <**4a** (N⌒N = bpy, 1269 Hz) ≪ **4g** (N⌒N = bpyr, 1296 Hz).

According to the greater *trans* influence of *P* ligands compared to *N* ligands [12] the resonances of the platinum-bound carbon atoms of **4** are high-field shifted and the values of coupling constants $^1J_{Pt,C}$ are increased compared to diacetylplatinum(II) complexes with *P* ligands (e.g. *cis*-[Pt(COMe)$_2$(PPh$_3$)$_2$], δ_C ($^1J_{Pt,C}$): 246.0 ppm (1037 Hz)) [7]. Comparison of the spectroscopic parameters of **4** with those of [Pt(COMe)(Cl)(N⌒N)] (**3**) showed that the chemical shifts in ^{1}H NMR and ^{13}C NMR spectra are in the same range but the coupling constants are different. Thus, the $^1J_{Pt,C}$ coupling constant in the acetyl chloro complex [Pt(COMe)Cl(bpy)] (989 Hz) is approximately 300 Hz lower than those in complex **4a** [3].

2.3. Structural characterization

2.3.1. General

Slow diffusion of diethyl ether into the reactions mixtures **4a**, **4c** and **4e** led to the formation of crystals **4a** · H$_2$O, **4c** and **4e** · H$_2$O suitable for X-ray diffraction analyses. Furthermore, diffusion of diethyl ether into a CHCl$_3$ solution of **4d** resulted in the formation of single crystals of **4d** · 1/2CHCl$_3$. In crystals of **4a** · H$_2$O and **4d** · 1/2CHCl$_3$ two symmetry independent molecules were found. Whereas both molecules **4d** in crystals of **4d** · 1/2CHCl$_3$ exhibited a very similar geometry, the geometric parameters for the symmetry independent molecules **4a** in crystals of **4a** · H$_2$O were found to differ more strongly. In Fig. 1 the asymmetric unit in crystals of **4a** · H$_2$O is shown. The molecular structures of **4c**, **4d** · 1/2CHCl$_3$ and **4e** · H$_2$O are shown in Figs. 2–4. Selected bond lengths and angles are collected in Table 2.

In all four complexes the platinum atoms showed a square-planar geometry having coordinated the chelating N⌒N ligand and two acetyl ligands. Inspection of the angles between the mean planes of the two halfs of the bipyridine ligands exhibited a remarkable twist of the bpy ligands in complexes **4c** (10.5(3)°) and **4e** · H$_2$O (12.3(4)°). Furthermore, only in complex **4d** · 1/2 CHCl$_3$ was found a coplanarity in good approximation between the mean bipyridine plane and the mean complex plane (interplanar angle: 2.1(5)/2.9(5)°). The acetyl ligands form angles with the complex planes between 32(1) and 87(1)°. Noteworthy, there were found two different arrangements: While in the complexes **4a** and **4c** the carbonyl oxygen atoms of the two acetyl ligands are orientated on the same side of the complex plane ("cisoid" conformation), they are on different sides of the complex plane in complexes **4d** and **4e** ("transoid" conformation).

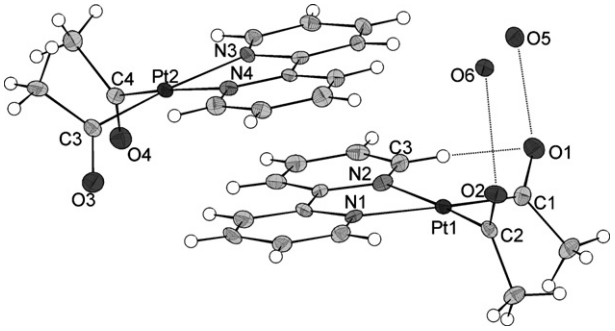

Fig. 1. Asymmetric unit of the crystal structure of [Pt(COMe)$_2$(bpy)] · H$_2$O (**4a** · H$_2$O). The thermal ellipsoids are drawn at a 30% probability level.

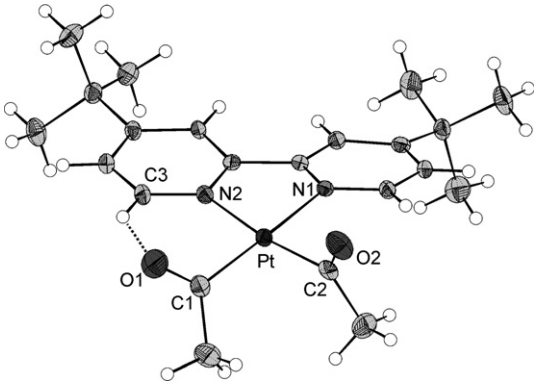

Fig. 2. Molecular structure of [Pt(COMe)$_2$(4,4′-*t*-Bu$_2$-bpy)] (**4c**). The thermal ellipsoids are drawn at a 30% probability level.

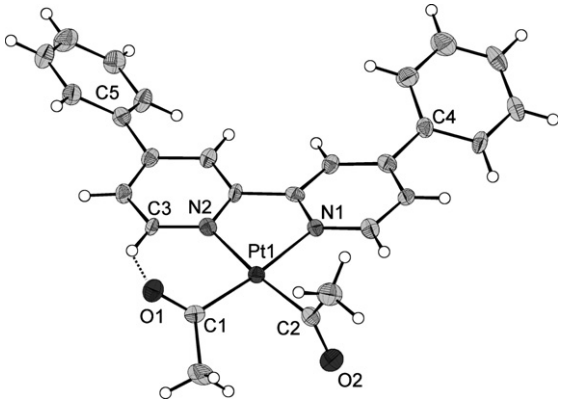

Fig. 3. Molecular structure of [Pt(COMe)$_2$(4,4′-Ph$_2$-bpy)] (**4d**) in crystals of **4d** · 1/2 CHCl$_3$. The thermal ellipsoids are drawn at a 30% probability level.

While the Pt–C-bond lengths (1.986(9)–2.040(6) Å) are in the range of other structurally characterized acylplatinum(II) complexes (median: 2.023 Å; lower/upper quartile 1.990/2.052 Å; number of observations n = 72 [13]) the C=O bond lengths (1.169(8)–1.26(1) Å) show a higher diversity (median: 1.220 Å; lower/upper quartile 1.193/1.235 Å; n = 72 [13]). All C=O bonds in **4a** (1.21(1)–1.23(1) Å) fall in this range whereas in the other complexes rather short (1.169(8) Å) and long (1.26(1) Å) C=O bonds were also found.

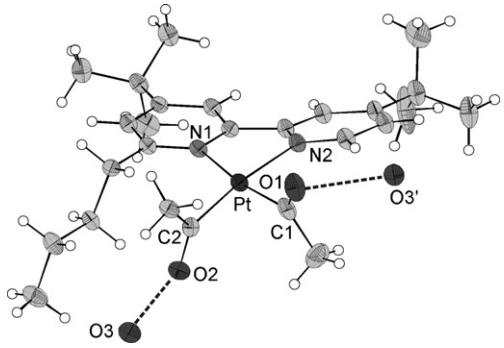

Fig. 4. Molecular structure of [Pt(COMe)$_2$(4,4′-*t*-Bu$_2$-6-*n*-Bu-bpy)] (**4e**) in crystals of **4e** · H$_2$O. The thermal ellipsoids are drawn at a 30% probability level.

Table 2
Selected bond length (in Å), bond angles (in °) and interplanar angles γ (in °)

	4a · H$_2$O[a]	**4c**	**4d** · 1/2CHCl$_3$[a]	**4e** · H$_2$O
Pt1–C1	1.99(1)/1.986(9)	1.998(6)	2.04(1)/2.09(1)	1.99(1)
Pt1–C2	1.991(8)/2.011(9)	2.040(6)	1.99(1)/1.99(1)	1.95(1)
C1–O1	1.22(1)/1.21(1)	1.187(9)	1.19(1)/1.17(1)	1.23(1)
C2–O2	1.22(1)/1.23(1)	1.169(8)	1.26(1)/1.24(1)	1.26(1)
C1–Pt1–C2	91.7(4)/88.2(4)	88.8(2)	89.5(4)/89.6(4)	82.2(4)
C2–Pt1–N1	95.6(3)/97.8(3)	97.2(2)	95.4(4)/96.1(4)	93.6(3)
N1–Pt1–N2	76.9(3)/77.0(3)	76.2(2)	76.6(3)/76.5(3)	76.5(3)
N2–Pt1–C1	95.9(4)/96.7(3)	98.1(2)	98.6(3)/98.0(3)	107.5(3)
γ(coord/MeC1=O1)	54.3(9)/84(0)	55.5(8)	38(1)/32(1)	79.3(9)
γ(coord/MeC2=O2)	78.2(9)/74(1)	83.9(7)	88(1)/86(1)	87(1)

[a] Values for the two symmetry independent molecules are separated by a slash.

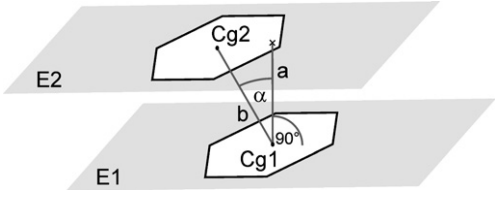

Fig. 5. Characteristic parameters of π–π stacking.

2.3.2. π–π stacking

In all four structures the packing of molecules in crystals can be rationalized in terms of π–π stacking and/or of the formation of hydrogen bonds. To describe π–π stacking in accord to Ref. [14] the following parameters have to be considered: the length of the ring normal of one ring to the plane formed by the other ring (*a*, Fig. 5), the centroid–centroid-distance (*b*), the angle between the ring normal and the centroid–centroid-vector (α), and the interplanar angle γ. These four parameters are listed in Table 3 for the relevant π–π interactions in the structures of **4a** · H$_2$O, **4c** and **4d** · 1/2CHCl$_3$.

Table 3
Distances of the planes *a* (in Å), Cg···Cg distances *b* (in Å), interplanar angles γ (in °) and angles between Cg–Cg vector and plane normal α (in °; see Fig. 5) for the π–π stackings in the structures of complexes **4**

	a	*b*	α	γ
*[Pt(COMe)$_2$(bpy)] · H$_2$O (**4a** · H$_2$O)*[a]				
A	3.40/3.40	3.72/3.69	24.1/22.7	5.2/2.2
B	3.37	3.65	22.4	1.8
C	3.47	3.60	15.6	2.2
*[Pt(COMe)$_2$(4,4′-t-Bu$_2$-bpy)] (**4c**)*				
	3.38	3.79	28.3	10.5
*[Pt(COMe)$_2$(4,4′-Ph$_2$-bpy)] · 1/2CHCl$_3$ (**4d** · 1/2CHCl$_3$)*				
	3.38/3.39	3.78/3.81	26.9/27.3	3.6/5.4

[a] Due to symmetry, types B and C stacking result in just one set of parameters whereas in type A stacking two sets were found.

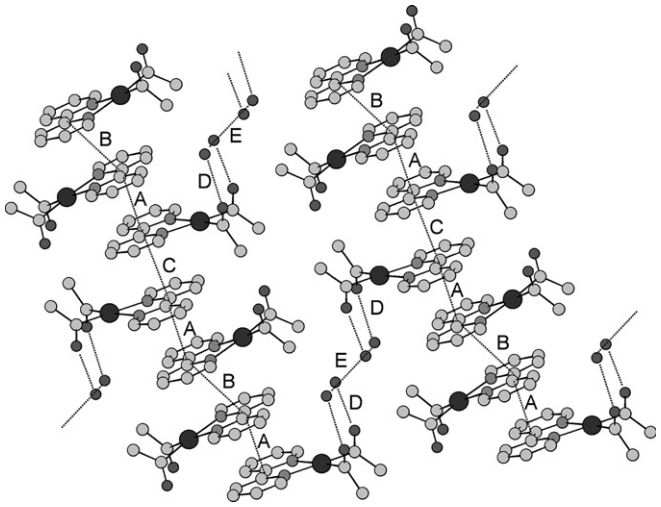

Fig. 6. Packing mode of [Pt(COMe)$_2$(bpy)] (**4a**) in crystals of **4a** · H$_2$O. Hydrogen atoms are omitted for clarity.

In crystals of **4a** · H$_2$O three different types of π–π stacking were found (Fig. 6, Table 3): Type A (see also Fig. 1) between two symmetry independent molecules, type B between two identical molecules that are not involved in hydrogen bonds and type C between two identical molecules that are involved in hydrogen bonds. Thus, the stacking mode can be described as ABACABAC... The parameters of the π–π stacking modes A, B and C in **4a** · H$_2$O are in the usual range of π–π stacking.

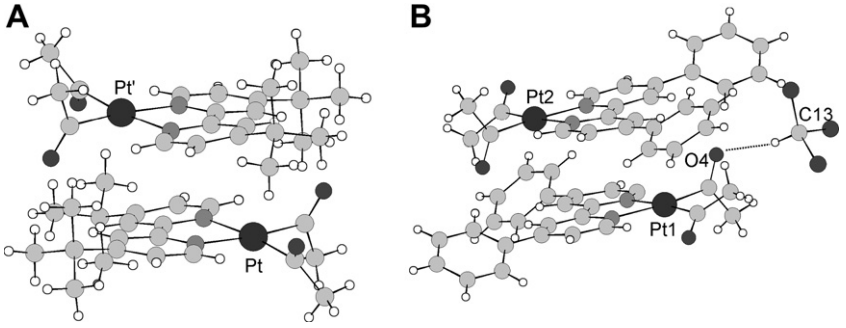

Fig. 7. Asymmetric units of the crystal structures of **4c** (A) and **4d** · 1/2CHCl$_3$ (B).

Table 4
Characteristic parameters of the C–H···O und O–H···O hydrogen bonds (distances in Å; angles in °) in the structures of complexes **4**

*[Pt(COMe)$_2$(bpy)] · H$_2$O (**4a** · H$_2$O)*						
C–H···O:	C3···O1	3.137(9)	O1···H	2.39	C3–H···O1	135
O–H···O:	O1···O5 (D)	2.789(9)	[a]			
	O2···O6 (D)	2.743(9)	[a]			
	O5···O6′ (E)	2.77(1)	[a]			
*[Pt(COMe)$_2$(4,4′-t-Bu$_2$-bpy)] (**4c**)*						
C–H···O:	C3···O1	3.180(9)	O1···H	2.43	C3–H···O1	136
*[Pt(COMe)$_2$(4,4′-Ph$_2$-bpy)] · 1/2CHCl$_3$ (**4d** · 1/2CHCl$_3$)*						
C–H···O:	C3···O1	3.06(1)	O1···H	2.34	C3–H···O1	133
	C8···O3	3.02(1)	O3···H	2.29	C8–H···O3	133
	C13···O4	3.17(1)	O4···H	2.20	C13–H···O4	163
*[Pt(COMe)$_2$(4,4′-t-Bu$_2$-6-n-Bu-bpy)] · H$_2$O (**4e** · H$_2$O)*						
O–H···O:	O1···O3′	2.81(1)				
	O2···O3	2.83(1)				

[a] The hydrogen atoms of the water molecules were not included in the solution of the crystal structure.

Complexes **4c** and **4d** · 1/2CHCl$_3$ are packed pairwise via π–π stacking (Fig. 7). Inspection of the angles α (Table 3) reveals a relatively strong shift (26.9–28.3°) likely due to the bulky *tert*-butyl substituents in **4c** and the phenyl groups in **4d** · 1/2CHCl$_3$, respectively.

Further π–π interactions in **4d** · 1/2CHCl$_3$ with centroid–plane distances of 3.69–3.78 Å, centroid–centroid distances of 4.08–4.45 Å and interplanar angles of 5.8–17.5° are found leading to a complex packing. In crystals of **4e** π–π stacking is not observed at all.

2.3.3. Hydrogen bonds

Complexes **4a**, **4d** and **4e** were found to crystallize with solvent molecules (H$_2$O, CHCl$_3$) giving rise to the formation of O–H···O and C–H···O hydrogen bonds, respectively (Table 4). In complex **4a** · H$_2$O two water molecules are connected through a hydrogen bond (Fig. 6, E; O···O 2.77(1) Å) and each of them acts as a hydrogen donor to an O atom of an acetyl ligand (Fig. 6, D; O···O 2.743(9)/2.789(9) Å). These hydrogen bonds link the columns formed by π–π stacking (Fig. 6). The O···O distances of type D and E hydrogen bonds are typically for analogous hydrogen bonds in water (e.g. H$_2$O: O···O 2.75–2.92 Å [15]) and between water and ketones (O···O 2.823(2) Å, [16]), respectively.

In the crystals of **4d** · 1/2CHCl$_3$ the solvate molecules act as H donors and the acetyl ligands as H acceptors in C–H···O hydrogen bonds (Fig. 7, B, Table 4). The C···O distance (3.17(1) Å) is characteristic for analogous hydrogen bonds formed between ketones and chloroform (mean C···O distance 3.18 [16]).

In crystals of [Pt(COMe)$_2$(4,4′-*t*-Bu$_2$-6-*n*-Bu-bpy)] · H$_2$O (**4e** · H$_2$O) the water molecules act as H donors and acetyl O atoms as H acceptors (C1=O1···H–O3–H···O2′=C2′) thus connecting two neighboured molecules **4e** (Fig. 4, Table 4). The O···O distances (2.81(1)/2.83(1) Å) are in the expected range for hydrogen bonds between water and ketones (O···O 2.823(2) Å, [16]). **4e** · H$_2$O crystallizes in the chiral space group $P6_2$. Thus, along the crystallographic *c*-axis a helical structure results in which the molecules of **4e** are connected through these hydrogen bonds (Fig. 8).

Furthermore, additionally to all these hydrogen bonds in which solvate molecules are involved, intramolecular C–H···O hydrogen bonds having aromatic C–H groups as donors and acetyl O atoms as acceptors were found. Most likely, these hydrogen bonds (C3–H···O1) in the structures of **4a** · H$_2$O, **4c** and **4d** · 1/2CHCl$_3$ (Figs. 1–3) give rise to a decrease of the interplanar angle between the acetyl ligand involved (MeC1=O1) and the complex plane by 20–50°. The geometrical parameters of these C3–H···O1 hydrogen bonds are in the expected range [16,17].

2.4. Conclusion

Reactions of the dinuclear platina-β-diketone **1** with chelating N⁀N donors resulting in an oxidative C–H addition followed by a reductive H–Cl elimination induced by OH$^-$ proved to be a straightforward synthesis for diacetylplatinum(II) complexes having N⁀N coligands in a wide variety (**4a**–**4j**). As the "parent" methyl complexes of this type, [PtMe$_2$(N⁀N)] (**5**), complexes **4** proved to be thermally stable and air-stable. Due to the higher electron density on platinum centre, complexes **5** were found to undergo oxidative addition reactions more readily than complexes **4** [18].

In the crystal structures of type **5** complexes, [PtMe$_2$(N⁀N)], the packing of the molecules is mainly dominated by π–π stacking of

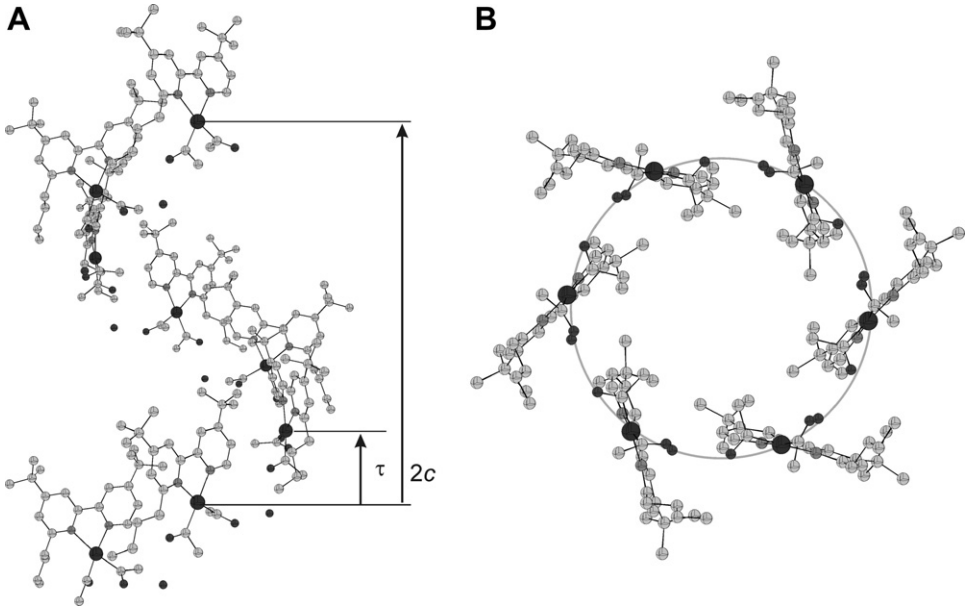

Fig. 8. (A) One strand of the double helix in the crystals of [Pt(COMe)$_2$(4,4′-*t*-Bu$_2$-6-*n*-Bu-bpy)] · H$_2$O (**4e** · H$_2$O). The hydrogen atoms are omitted for clarity. (B) View along the crystallographic *c*-axis.

the aromatic ring systems [19]. Additionally to π–π stacking in type **4** complexes the formation of hydrogen bonds was found to be a structure giving motif. This might be caused by the ability of the oxygen atoms of the acetyl ligands to act as hydrogen bond acceptors.

3. Experimental

3.1. General comments

All reactions were performed under an argon atmosphere using the standard Schlenk techniques. Solvents were dried (Et_2O over Na/benzophenone, CH_2Cl_2 over CaH_2) and distilled prior to use. NMR spectra were recorded on Varian spectrometers Gemini 200, VXR 400 and Unity 500 operating at 200, 400 and 500 MHz for ^1H, respectively. Solvent signals (^1H, ^{13}C) were used as internal references. When necessary, assignments were revealed by running ^1H–^1H and ^1H–^{13}C COSY NMR experiments. IR spectra were recorded on a Galaxy Mattson 5000 FT-IR spectrometer using KBr pellets. Microanalyses were performed by the University of Halle microanalytical laboratory using CHNS-932 (LECO) and Vario EL (Elementaranalysensysteme) elemental analysers. The complex $[Pt_2\{(COMe)_2H\}_2(\mu\text{-}Cl)_2]$ (**1a**) was prepared according to a published method [2].

3.2. Synthesis of [Pt(COMe)$_2$Cl(H)(N⌒N)] (**2a–j**)

According to Ref. [3], complexes **2a–j** were prepared by the addition of the corresponding N⌒N ligand (0.32 mmol) to a solution of **1a** (100 mg, 0.16 mmol) in CH_2Cl_2 (10 ml) at −78 °C. After stirring for 30 min at this temperature, the solution was warmed to 0 °C and stirred for additional 30 min. Then, the solvent was removed under reduced pressure. The residue was dissolved in CH_2Cl_2 (ca. 2 ml) and Et_2O (ca. 5 ml) was added. The precipitate formed was filtered, washed with Et_2O (2 × 2 ml) and dried in vacuum.

Yield: 70–90%. The identities of the products were confirmed by comparison with ^1H NMR data given in Ref. [3].

3.3. Synthesis of [Pt(COMe)$_2$(N⌒N)] (**4a–j**)

To a solution of [Pt(COMe)$_2$Cl(H)(N⌒N)] (**2**) (0.1 mmol) in CH_2Cl_2 (20 ml) an aqueous solution of NaOH (20 mg in 10 ml) was added. After vigorously stirring for approximately 30 min the colour of the organic layer became red. The phases were separated and the aqueous phase was extracted with CH_2Cl_2 (2 × 10 ml). The combined organic extracts were dried with $NaSO_4$, filtered and the solvent was removed under reduced pressure. The residue was dissolved in CH_2Cl_2 (ca. 2 ml) and *n*-pentane (ca. 5 ml) was added. The precipitate obtained was filtered, washed with *n*-pentane (2 × 2 ml) and dried in vacuum over P_4O_{10}.

3.3.1. [Pt(COMe)$_2$(bpy)] (**4a**)

Yield: 175 mg (85%). Anal. Calc. for $C_{14}H_{14}N_2O_2Pt$ (437.4 g/mol): C, 38.44; H, 3.23; N, 6.41. Found: C, 38.20; H, 3.01; N, 6.32%. ^1H NMR ($CDCl_3$, 400 MHz): δ 2.34 (s + d, $^3J_{Pt,H}$ = 22.7 Hz, 6H, COC*H*$_3$), 7.54 (m, 2H, *H*5/5′ of bpy), 8.04 (m, 4H, *H*3/3′, *H*4,4′ of bpy), 8.86 (m, 2H, *H*6/6′ of bpy). ^{13}C NMR ($CDCl_3$, 125 MHz): δ 44.4 (s + d, $^2J_{Pt,C}$ = 371 Hz, COCH$_3$), 121.9 (s, *C*3/3′ of bpy), 126.8 (s, *C*5/5′ of bpy), 138.7 (s, *C*4/4′ of bpy), 151.2 (s, *C*2/2′ of bpy), 155.1 (s, *C*6/6′ of bpy), 230.1 (s + d, $^1J_{Pt,C}$ = 1269 Hz, Pt–*C*). IR: ν (cm^{-1}) 3060(w), 2970(w), 2898(w), 1606(s), 1581(s), 1558(m), 1473(m), 1446(m), 1413(m), 1334(m), 1319(m), 1166(w), 1110(m), 1090(m), 1016(w), 930(w), 762(s), 727(m), 601(w).

3.3.2. [Pt(COMe)$_2$(4,4′-Me$_2$-bpy)] (**4b**)

Yield: 165 mg (80%). Anal. Calc. for $C_{16}H_{18}N_2O_2Pt$ (465.4 g/mol): C, 41.29; H, 3.90; N, 6.02. Found: C, 41.15; H, 4.05; N, 6.06%. ^1H NMR ($CDCl_3$, 400 MHz) δ 2.21 (s + d, $^3J_{Pt,H}$ = 23.7 Hz, 6H, COC*H*$_3$), 2.39 (s, 6H, bpy-C*H*$_3$), 7.15 (m, 2H, *H*5,5′ of bpy), 7.79 (m, 2H, *H*3,3′ of bpy), 8.83 (m, 2H, *H*6,6′ of bpy). ^{13}C NMR ($CDCl_3$, 400 MHz) δ 21.6 (s, bpy-*C*H$_3$), 44.4 (s + d, $^2J_{Pt,C}$ = 370 Hz, COCH$_3$), 122.9 (s, *C*3,3′ of bpy), 127.1 (s, *C*5,5′ of bpy), 150.0 (s, *C*4,4′ of bpy), 150.7 (s, *C*6,6′ of bpy), 154.6 (s, *C*2,2′ of bpy), 230.6 (s + d, $^3J_{Pt,C}$ = 1265 Hz, Pt–*C*). IR: ν (cm^{-1}) 3066(w), 2962(w), 2886(w), 1614(s), 1590(s), 1485(w), 1442(m), 1413(m), 1334(w), 1243(w), 1107(m), 1088(m), 1024(w), 924(w), 831(m), 606(w).

3.3.3. [Pt(COMe)$_2$(4,4′-t-Bu$_2$-bpy)] (**4c**)

Yield: 180 mg (70%). Anal. Calc. for $C_{22}H_{30}N_2O_2Pt$ (549.6 g/mol): C, 48.08; H, 5.50; N, 5.10. Found: C, 48.51; H, 5.83; N, 5.19%. ^1H NMR (400 MHz, $CDCl_3$) δ 1.34 (s, 18H, C(C*H*$_3$)$_3$), 2.26 (s + d, $^3J_{Pt,H}$ = 24.3 Hz, 6H, COC*H*$_3$), 7.43 (m, 2H, *H*5,5′ of bpy), 7.89 (m, 2H, *H*3,3′ of bpy), 8.62 (m, 2H, *H*6,6′ of bpy). ^{13}C NMR (100 MHz, $CDCl_3$) δ 30.1 (s, C(*C*H$_3$)$_3$), 35.4 (s, *C*(CH$_3$)$_3$), 44.4 (s + d, $^2J_{Pt,C}$ = 374 Hz, COCH$_3$), 118.5 (s, *C*3,3′ of bpy), 123.8 (s, *C*5,5′ of bpy), 150.5 (s, *C*6,6′ of bpy), 155.1 (s, *C*2,2′ of bpy), 163.5 (s, *C*4,4′ of bpy), 231.3 (s + d, $^3J_{Pt,C}$ = 1263 Hz, Pt–*C*). IR: ν (cm^{-1}) 3074(w), 2962(m), 2906(m), 2870(w), 1618(s), 1591(s), 1481(m), 1465(m), 1411(m), 1365(w), 1324(w), 1252(w), 1103(m), 1020(w), 928(w), 900(w), 876(w), 841(w), 605(w).

3.3.4. [Pt(COMe)$_2$(4,4′-Ph$_2$-bpy)] (**4d**)

Yield: 240 mg (85%). Anal. Calc. for $C_{26}H_{22}N_2O_2Pt$ (589.5 g/mol): C, 52.87; H, 3.76; N, 4.75. Found: C, 52.45; H, 3.62; N, 4.82%. ^1H NMR (400 MHz, $CDCl_3$) δ 2.28 (s + d, $^3J_{Pt,H}$ = 23.8 Hz, 6H, COC*H*$_3$), 7.52 (m, 6H, *p*-Ph, *o*-Ph), 7.60 (m, 2H, *H*5,5′ of bpy), 7.70 (m, 4H, *m*-Ph), 8.28 (m, 2H, *H*3,3′ of bpy), 8.74 (m, 2H, *H*6,6′ of bpy). ^{13}C NMR (100 MHz, $CDCl_3$) δ 44.4 (s + d, $^2J_{Pt,C}$ = 370 Hz, COCH$_3$), 120.0 (s, *C*3,3′ of bpy), 124.4 (s, *C*5,5′ of bpy), 127.1 (s, *m*-Ph), 129.6 (s, *o*-Ph), 130.5 (s, *p*-Ph), 136.3 (s, *C*4,4′ of bpy), 151.2 (s, *i*-Ph), 151.4 (s, *C*6,6′ of bpy), 155.5 (s, *C*2,2′ of bpy), 230.4 (s + d, $^3J_{Pt,C}$ = 1262 Hz, Pt–*C*). IR: ν (cm^{-1}) 3055(w), 2975(w), 1662(w), 1610(s), 1581(s), 1544(w), 1475(w), 1408(m), 1331(w), 1100(m), 1089(m), 1016(w), 926(w), 849(w), 761(m), 695(m), 627(w), 592(w).

3.3.5. [Pt(COMe)$_2$(4,4′-t-Bu$_2$-6-n-Bu-bpy)] (**4e**)

Yield: 175 mg (60%). Anal. Calc. for $C_{26}H_{38}N_2O_2Pt$ (605.7 g/mol): C, 51.56; H, 6.32; N, 4.63. Found: C, 50.98; H, 6.09; N, 4.91%. ^1H NMR (200 MHz, $CDCl_3$) δ 0.81 (t, 3H, CH_2CH_3), 1.23 (m, 2H, CH_2CH_3),1.28 (s, 18H, C(C*H*$_3$)$_3$), 1.54 (m, 2H, $CH_2CH_2CH_3$), 2.17 (s + d, $^3J_{Pt,H}$ = 24.4 Hz, 3H, COC*H*$_3$), 2.27 (s + d, $^3J_{Pt,H}$ = 20.5 Hz, 3H, COC*H*$_3$), 2,74 (m, 2H, bpy-C*H*$_2$), 7.27 (m, 2H, *H*5,5′ of bpy), 7.71 + 7.79 (m, 2H, *H*3,3′ of bpy), 8.46 (m, 1H, *H*6′ of bpy). ^{13}C NMR (125 MHz, $CDCl_3$) δ 13.8 (s, CH_2CH_3), 22.0 (s, CH_2CH_3), 30.1 (s, C(CH$_3$)$_3$), 31.9 (s, $CH_2CH_2CH_3$), 35.1 + 35.4 (s, *C*(CH$_3$)$_3$), 39.9 (s, bpy-CH_2), 42.2 (s + d, $^2J_{Pt,C}$ = 378 Hz, COCH$_3$), 44.7 (s + d, $^2J_{Pt,C}$ = 358 Hz, COCH$_3$), 116.5 + 119.3 (s, *C*3,3′ of bpy), 122.7 + 123.2 (s, *C*5,5′ of bpy), 149.5 (s, *C*6′ of bpy), 155.5 + 156.3 (s, *C*2,2′ of bpy), 163.1 + 163.2 (s, *C*4,4′ of bpy), 165.9 (s, *C*6 of bpy), 225.8 (s + d, $^3J_{Pt,C}$ = 1250 Hz, Pt–*C*), 232.8 (s + d, $^3J_{Pt,C}$ = 1244 Hz, Pt–*C*). IR: ν (cm^{-1}) 3081(w), 2960(s), 2870(m), 1616(s), 1547(m), 1460(m), 1423(m), 1363(m), 1309(m), 1257(w), 1105(m), 1016(w), 925(w), 906(w), 734(w), 692(w), 598(w).

3.3.6. [Pt(COMe)$_2$(bpym)] (**4f**)

Yield: 165 mg (80%). Anal. Calc. for $C_{12}H_{12}N_4O_2Pt$ (439.3 g/mol): C, 32.81; H, 2.75; N, 12.75. Found: C, 32.46; H, 2.88; N, 12.38%. ^1H NMR ($CDCl_3$, 200 MHz) δ 2.32 (s + d, $^3J_{Pt,H}$ = 28.0 Hz, 6H, COC*H*$_3$), 7,69 (m, 2H, *H*5,5′ of bpym), 9.20 (m, 4H, *H*4,4′ + *H*6,6′ of bpym).

^{13}C NMR ($CDCl_3$, 100 MHz) δ 44.2 (s + d, $^2J_{Pt,C}$ = 386 Hz, $COCH_3$), 123.7 (s, *C*5,5′ of bpym), 157.7 + 159.1 (s, *C*4,4′ + *C*6,6′ of bpym), 161.6 (s, *C*2,2′ of bpym), 226.6 (s + d, $^3J_{Pt,C}$ = 1244 Hz, Pt–*C*). IR: ν (cm^{-1}) 3074(m), 2964(w), 1620(s), 1581(s), 1409(s), 1330(m), 1260(w), 1105(m), 1012(w), 943(w), 920(w), 820(w), 752(m), 661(m), 606(w).

3.3.7. [Pt(COMe)$_2$(bpyr)] (**4g**)

Yield: 160 mg (75%). Anal. Calc. for $C_{12}H_{12}N_4O_2Pt$ (439.3 g/mol): C, 32.81; H, 2.75; N, 12.75. Found: C, 32.54; H, 2.81; N, 12.67%. ^{1}H NMR ($CDCl_3$, 400 MHz) δ 2.33 (s + d, $^3J_{Pt,H}$ = 27.8 Hz, 6H, $COCH_3$), 8.98 (m, 4H, *H*3,3′ + *H*5,5′ of bpyr), 9.52 (m, 2H, *H*6,6′ of bpyr). ^{13}C-NMR ($CDCl_3$, 100 MHz) δ 44.0 (s + d, $^2J_{Pt,C}$ = 385 Hz, $COCH_3$), 143.6 (s, *C*3,3′ of bpyr) 144.5 (s, *C*5,5′ of bpyr), 147.9 (s, *C*2,2′ of bpyraz), 149.0 (s, *C*6,6′ of bpyr), 226.3 (s + d, $^3J_{Pt,C}$ = 1296 Hz, Pt–C). IR: ν (cm^{-1}) 3053(w), 3032(w), 2972(w), 2897(w), 1731(w), 1587(s), 1471(w), 1410(m), 1333(w), 1155(m), 1111(m), 1041(m), 928(w), 849(w), 605(w), 474(w), 453(w).

3.3.8. [Pt(COMe)$_2$(phen)] (**4h**)

Yield: 175 mg (80%). Anal. Calc. for $C_{16}H_{14}N_2O_2Pt$ (461.4 g/mol): C, 41.65; H, 3.06; N, 6.07. Found: C, 41.98; H, 3.19; N, 5.91%. ^{1}H NMR (400 MHz, $CDCl_3$) δ 2.40 (s + d, $^3J_{Pt,H}$ = 21.2 Hz, 6H, CH_3), 7,82 (m, 2H, *H*3 + *H*8 of phen), 8,04 (m, 2H, *H*5 + *H*6 of phen), 8,50 (m, 2H, *H*4 + *H*7 of phen), 9.11 (m, 2H, *H*2 + *H*9 of phen). ^{13}C NMR (100 MHz, $CDCl_3$) δ 44.6 (s + d, $^2J_{Pt,C}$ = 385 Hz, CH_3), 125.3 (s, *C*3 + *C*8 of phen) 127.3 (s, *C*5 + *C*6 of phen), 129.9 (s, *C*10a + *C*10b of phen), 137.9 (s, *C*4 + *C*7 of phen), 146.3 (s, *C*4a + *C*6a of phen), 151.3 (s, *C*2 + *C*9 of phen), 230.1 (s + d, $^3J_{Pt,C}$ = 1274 Hz, Pt–*C*). IR: ν (cm^{-1}) 3079(w), 2979(w), 2898(w), 1610(s), 1583(s), 1512(m), 1429(m), 1329(m), 1109(m), 928(w), 843(m), 717(m), 607(w).

3.3.9. [Pt(COMe)$_2$(4-Me-phen)] (**4i**)

Yield: 170 mg (75%). Anal. Calc. for $C_{17}H_{16}N_2O_2Pt$ (475.4 g/mol): C, 42.95; H, 3.39; N, 5.89. Found: C, 42.45; H, 3.21; N, 5.93%. ^{1}H NMR (400 MHz, $CDCl_3$) δ 2.32 (s + d, $^3J_{Pt,H}$ = 25.1 Hz, 6H, $COCH_3$), 5.31 (s, 3H, phen-CH_3), 7.60 + 7.80 (m, 2H, *H*3 + *H*8 of phen), 7.92 + 8.06 (m, 2H, *H*5 + *H*6 of phen), 8.50 (m, 1H, *H*7 of phen), 8.85 + 9.04 (m, 2H, *H*2 + *H*9 of phen). ^{13}C NMR (100 MHz, $CDCl_3$) δ 19.6 (s, phen-CH_3), 44.5 (s + d, $^2J_{Pt,C}$ = 386 Hz, $COCH_3$), 124.1 + 127.2 (s, *C*3 + *C*8 of phen) 125.4. + 126.3 (s, *C*10a + *C*10b of phen), 130.8 (s, *C*7 of phen), 138.1 (s, *C*5 + *C*6 of phen), 146.3 + 146.8 (s, *C*4a + *C*6a of phen), 148.4 (s, *C*4 of phen), 150.8 + 151.5 (s, *C*2 + *C*9 of phen), 227.7 + 227.8 (s, Pt–*C*). IR: ν (cm^{-1}) 3078(w), 2966(w), 2897(w), 1589(s), 1516(m), 1423(m), 1325(w), 1227(w), 1103(m), 916(w), 835(w), 721(w), 604(w).

3.3.10. [Pt(COMe)$_2$(5-Me-phen)] (**4j**)

Yield: 175 mg (75%). Anal. Calc. for $C_{17}H_{16}N_2O_2Pt$ (475.4 g/mol): C, 42.95; H, 3.39; N, 5.89. Found: C, 42.82; H, 3.29; N, 6.01%. ^{1}H NMR (400 MHz, $CDCl_3$) δ 2.32 (s + d, $^3J_{Pt,H}$ = 25.3 Hz, 6H, $COCH_3$), 5.32 (s, 3H, phen-CH_3), 7.71 (m, 1H, *H*6 of phen), 7.80 + 7.86 (m, 2H, *H*3 + *H*8 of phen), 8.42 + 8.63 (m, 2H, *H*4 + *H*7 of phen), 8.99 + 9.07 (m, 2H, *H*2 + *H*9 of phen). ^{13}C NMR δ (100 MHz, $CDCl_3$) 18.7 (s, phen-CH_3), 44.5 (s + d, $^2J_{Pt,C}$ = 387 Hz, $COCH_3$), 124.9 + 125.2 (s, *C*3 + *C*8 of phen) 126.1 (s, *C*6 of phen), 129.7 + 130.2 (s, *C*10a + *C*10b of phen), 134.7 + 137.0 (s, *C*4 + *C*7 of phen), 135.0 (s, *C*5 of phen), 145.6 + 146.5 (s, *C*4a + *C*6a of phen), 150.2 + 150.7 (s, *C*2 + *C*9 of phen), 227.2 + 227.8 (s, Pt–*C*). IR: ν (cm^{-1}) 3072(w), 2974(w), 2899(w), 1616(m), 1589(s), 1518(w), 1423(m), 1328(w), 1219(w), 1107(m), 931(w), 871(w), 798(w), 724(w), 602(w).

3.4. X-ray crystallography

Single crystals suitable for X-ray diffraction measurements were obtained by recrystallisation from methylene chloride/diethyl ether (1:2) (**4a** · H_2O, **4c**, **4e** · H_2O) and by recrystallisation from chloroform/pentane (1:1) (**4d** · 1/2$CHCl_3$), respectively. Intensity data were collected on a STOE IPDS 2 at 153(2) K (**4a** · H_2O, **4c**, **4e** · H_2O) and 133(2) K (**4d** · 1/2$CHCl_3$), respectively, with Mo Kα radiation (λ = 0.71073 Å, plane graphite monochromator). Absorption corrections were applied numerically (T_{min}/T_{max} 0.075/0.232, **4a** · H_2O; T_{min}/T_{max} 0.221/0.480, **4c**; T_{min}/T_{max} 0.191/0.794, **4d** · 1/2$CHCl_3$; T_{min}/T_{max} 0.214/0.725, **4e** · H_2O). The crystallographic data and structure refinement parameters are listed in Table 5. All structures were solved by direct methods with SHELXS-97 and refined using full-matrix least-square routines against F^2 with SHELXL-97 [20]. Non-hydrogen atoms were refined with anisotropic and hydrogen atoms with isotropic displacement parameters. Hydrogen atoms were refined according the "riding model".

Table 5
Crystallographic and data collection parameters for compounds **4a** · H_2O, **4c**, **4d** · 1/2$CHCl_3$ and **4e** · H_2O

	4a · H_2O	**4c**	**4d** · 1/2$CHCl_3$	**4e** · H_2O
Empirical formula	$C_{28}H_{32}N_4O_6Pt_2$	$C_{22}H_{30}N_2O_2Pt$	$C_{53}H_{45}Cl_3N_4O_4Pt_2$	$C_{26}H_{40}N_2O_3Pt$
M_r	910.8	549.6	1298.5	623.7
Crystal system	Triclinic	Monoclinic	Orthorhombic	Hexagonal
Space group	$P\bar{1}$	$P2_1/n$	$P2_12_12_1$	$P6_2$
a (Å)	10.054(2)	11.192(1)	14.273(1)	20.575(1)
b (Å)	11.012(3)	12.932(1)	11.8988(5)	20.575(1)
c (Å)	13.841(3)	14.933(1)	28.273(1)	11.6908(6)
α (°)	110.89(2)	90	90	90
β (°)	92.46(2)	96.048(7)	90	90
γ (°)	103.19(2)	90	90	120
V (Å^3)	1380.9(5)	2149.3(3)	4801.6(5)	4286.0(4)
Z	2	4	4	6
D_{calc} (g cm^{-1})	2.190	1.698	1.796	1.450
μ (Mo Kα) (mm^{-1})	10.169	6.546	6.038	4.936
θ Range (°)	1.59–25.00	2.09–25.50	1.44–25.00	1.98–25.49
Number of reflections collected	9018	14314	31241	17001
Number of reflections observed [$I > 2\sigma(I)$]	4102	3615	3798	4209
Number of independent reflections	4578	4001	4711	4736
Number of data/restraints/parameters	4578/0/365	4001/0/253	4711/0/600	4736/1/302
Goodness-of-fit on F^2	1.065	1.157	0.939	1.017
R_1, wR_2 [$I > 2\sigma(I)$]	0.0493, 0.1222	0.0297, 0.0731	0.0278, 0.0602	0.0421, 0.0895
R_1, wR_2 (all data)	0.0529, 0.1244	0.0342, 0.0744	0.0405/0.0627	0.0361, 0.0879
Largest difference peak and hole (e Å^{-3})	4.441/−5.132	1.078/−1.165	1.163/−1.676	0.669/−0.528

Acknowledgement

We gratefully acknowledge support by the Deutsche Forschungsgemeinschaft. We also thank Merck (Darmstadt) for gifts of chemicals.

Appendix A. Supplementary material

CCDC 677227, 677228, 677229 and 677230 contain the supplementary crystallographic data for **4a** · H_2O, **4c**, **4d** · 1/2$CHCl_3$ and **4e** · H_2O. These data can be obtained free of charge from The Cambridge Crystallographic Data Centre via www.ccdc.cam.ac.uk/data_request/cif. Supplementary data associated with this article can be found, in the online version, at doi:10.1016/j.jorganchem.2008.04.016.

References

[1] D. Steinborn, Dalton Trans. (2005) 2664.
[2] (a) M. Gerisch, F.W. Heinemann, C. Bruhn, J. Scholz, D. Steinborn, Organometallics 18 (1999) 564;
(b) C. Albrecht, C. Wagner, K. Merzweiler, T. Lis, D. Steinborn, Appl. Organomet. Chem. 19 (2005) 1155.
[3] M. Gerisch, C. Bruhn, A. Vyater, J.A. Davies, D. Steinborn, Organometallics 17 (1998) 3101.
[4] (a) G.S. Hill, L.M. Rendina, R.J. Puddephatt, Organometallics 14 (1995) 4966;
(b) S.S. Stahl, J.A. Labinger, J.E. Bercaw, J. Am. Chem. Soc. 118 (1996) 5961.
[5] A. Vyater, C. Wagner, K. Merzweiler, D. Steinborn, Organometallics 21 (2002) 4369.
[6] T. Gosavi, E. Rusanov, H. Schmidt, D. Steinborn, Inorg. Chim. Acta 357 (2004) 1781.
[7] C. Albrecht, Ph.D. Thesis, Martin-Luther-Universität Halle-Wittenberg, 2006.
[8] R.J. Klingler, J.C. Huffman, J.K. Kochi, J. Am. Chem. Soc. 104 (1982) 2147.
[9] L.M. Redina, R.J. Puddephatt, Chem. Rev. 97 (1997) 1735.
[10] D. Steinborn, A. Vyater, C. Bruhn, M. Gerisch, H. Schmidt, J. Organomet. Chem. 597 (2000) 10.
[11] V. Barone, C. Cauletti, M.N. Piancastelli, M. Ghedini, M. Toscano, J. Phys. Chem. 95 (1991) 7217.
[12] T.G. Appleton, H.C. Clark, L.E. Manzer, Coord. Chem. Rev. 10 (1973) 335.
[13] Cambridge Structural Database (CSD), Cambridge University Chemical Laboratory, Cambridge, 2006.
[14] C. Janiak, J. Chem. Soc., Dalton Trans. (2000) 3885.
[15] G.A. Jeffrey, W. Saenger, Hydrogen Bonding in Biological Structures, Springer, Berlin, 1991.
[16] (a) T. Steiner, New J. Chem. 22 (1998) 1099;
(b) G.R. Desiraju, T. Steiner, The Weak Hydrogen Bond, Oxford University Press, Oxford, 1999.
[17] (a) D. Braga, F. Grepioni, Acc. Chem. Res. 30 (1997) 81;
(b) D. Braga, F. Grepioni, K. Biradha, V.R. Pedireddi, G.R. Desiraju, J. Am. Chem. Soc. 117 (1995) 3156.
[18] M. Werner, Ph.D. Thesis, Martin-Luther-Universität Halle-Wittenberg, 2008.
[19] (a) S. Achar, V.J. Catalano, Polyhedron 16 (1997) 1555;
(b) A. Klein, J. van Slageren, S. Zalis, Eur. J. Inorg. Chem. (2003) 1917;
(c) G.J.P. Britovsek, R.A. Taylor, G.J. Sunley, D.J. Law, A.J.P. White, Organometallics 25 (2006) 2074.
[20] G.M. Sheldrick, SHELXS-97, SHELXL-97, Programs for Crystal Structure Determination, Universität Göttingen, 1990/1997.